



# A renewable power system for an off-grid sustainable telescope fueled by solar power, batteries and green hydrogen

Isabelle Viole<sup>\*,1</sup>, Guillermo Valenzuela-Venegas<sup>1</sup>, Marianne Zeyringer, Sabrina Sartori

Department of Technology Systems (ITS), University of Oslo, Gunnar Randars Vei 19, 2007 Kjeller, Norway

## ARTICLE INFO

### Keywords:

Power system optimization  
Hybrid energy storage  
Off-grid  
Green hydrogen  
Carbon footprint

## ABSTRACT

A large portion of astronomy's carbon footprint stems from fossil fuels supplying the power demand of astronomical observatories. Here, we explore various isolated low-carbon power system setups for the newly planned Atacama Large Aperture Submillimeter Telescope, and compare them to a business-as-usual diesel power generated system. Technologies included in the designed systems are photovoltaics, concentrated solar power, diesel generators, batteries, and hydrogen storage. We adapt the electricity system optimization model highRES to this case study and feed it with the telescope's projected energy demand, cost assumptions for the year 2030 and site-specific capacity factors. Our results show that the lowest-cost system with LCOEs of \$116/MWh majorly uses photovoltaics paired with batteries and fuel cells running on imported and on-site produced green hydrogen. Some diesel generators run for backup. This solution would reduce the telescope's power-side carbon footprint by 95% compared to the business-as-usual case.

## 1. Introduction

To contribute to the global effort limiting the global rise in temperature below 1.5°, astronomers need to reduce their carbon footprint. Today's carbon footprint per astronomer is estimated at ~37 t CO<sub>2</sub> equivalents (CO<sub>2</sub>e) annually [1,2]. The sector as a whole emits ~1200 kt CO<sub>2</sub>e per annum, that is 0.0024% of the global greenhouse gas (GHG) emissions (50.2 Gt in 2020). This exceeds the population share of this group by more than a factor of six, since just 30,000 out of the current population of 8 bn are astronomers [2]. Next to CO<sub>2</sub>e emissions related to flights and powering supercomputers, 13% stems from powering the operation of observatories [1]. These have high power needs for the cryogenic cooling of instruments and the motors tracking their dishes. As most of this electricity stems from fossil fuel sources today, ground-based telescopes have a median carbon intensity of 24 t CO<sub>2</sub>e per paper published using their generated data [2]. For comparison, the carbon footprint per capita in the European Union was 6.8t CO<sub>2</sub>e in the year 2019 [3].

Growing awareness of climate change mitigation and volatile prices of fossil fuels led some observatories to subsequently add Renewable Energy Sources (RES) to their power generation. In Hawaii, the Gemini Observatory supplies 10% of its demand with solar photovoltaic (PV) arrays since 2015. In the Chilean Atacama Desert, the La Silla observatory is powered by more than 50% solar energy since 2016 and the Paranal observatory commissioned PV arrays in 2022 [4–6].

Due to the decades-long lifetime of astronomical research infrastructures, decisions taken on power supply in new projects today lock in CO<sub>2</sub>e emissions for decades. To strive for lower carbon footprints, AtLAST – The Atacama Large Aperture Submillimeter Telescope – is the first observatory already including plans for a power system powered by RES in its design stage [7]. AtLAST is a design study project for a 50 m single dish submillimeter/millimeter telescope on the Chajnantor plateau in the Atacama, at an elevation of ~5000 m [7,8]. It is planned to start its operation in the early 2030s. The very high and dry site is necessary to minimize water vapor in the atmosphere, which absorbs submillimeter photons. The eleven neighboring telescopes, like the Atacama Pathfinder Experiment (APEX) and the Atacama Large Millimeter/submillimeter Array (ALMA), today rely on fossil fuels to meet their power demands.

Several recent studies carried out simulations and techno-economic assessments to decarbonize islanded stationary systems for household demands, considering present-day component costs: Endo et al. [9] simulated the operation of a stationary system to power a residential building, consisting of RES, an electrolyzer, a hydrogen (H<sub>2</sub>) storage system in metal hydrides (MH), a proton-exchange membrane fuel cell (PEMFC) and batteries. They showed that PV and PEMFC generation can meet most of the demand during fine and cloudy weather. Ghenai et al. techno-economically optimized an off-grid solar PV and H<sub>2</sub> energy system to meet the 500 kWh daily demand of a desert community,

\* Corresponding author.

E-mail addresses: [isabelle.viole@its.uio.no](mailto:isabelle.viole@its.uio.no) (I. Viole), [guillermo.valenzuela@its.uio.no](mailto:guillermo.valenzuela@its.uio.no) (G. Valenzuela-Venegas).

<sup>1</sup> These authors contributed equally to this work.

**Abbreviations**

\$ <sub>2020</sub>	real2020-\$, inflation adjusted US dollar value to the year 2020; all \$ values in this work without indexed year are set to real2022-\$
ALMA	Atacama Large Millimeter/submillimeter Array
APEX	Atacama Pathfinder Experiment
AtLAST	Atacama Large Aperture Submillimeter Telescope
CAPEX	Capital expenditures
CO <sub>2</sub> e	Carbon dioxide equivalent
CSP	Concentrated solar power
DOE	US-American Department of Energy
H <sub>2</sub>	Hydrogen
IEA	International Energy Agency
IRENA	International Renewable Energy Agency
kW <sub>e</sub>	kilowatt, electric
kWh <sub>th</sub>	kilowatt-hour, thermal
kW <sub>p</sub>	kilowatt-peak, unit for photovoltaic nominal power
LCOE	Levelized costs of electricity
Li-ion	Lithium-ion
MH	Metal hydrides
NREL	National Renewable Energy Laboratory
OPEX	Operational expenditures
PEM	Proton-exchange membrane
PEMFC	PEM fuel cell
pp.	percentage points
PV	Solar photovoltaic
PT	Parabolic trough, a CSP generation system
RES	Renewable Energy Sources
ST	Solar tower, a CSP generation system

**Scenarios:**

BAU	Business-as-usual: Only diesel generators on-site at an altitude of 5000 m
CSP	CSP at 2500 m
PVD↑	PV and Diesel: Using PV and diesel generation at 5000 m
PVD↓	PV and Diesel at 2500 m
PVDES↑	PV, Diesel and Energy Storage: Using PV generation, a hybrid energy storage system and backup diesel generation at 5000 m
PVDES↓	PV, Diesel and Energy Storage at 2500 m
RES↑	All Renewables: Using PV generation and a hybrid energy storage system at 5000 m
RES↓	All Renewables at 2500 m

resulting in levelized costs of electricity (LCOE) of \$145/MWh [10]. Gebrehiwot et al. similarly analyzed a hybrid power system with PV, wind, and diesel generation plus batteries to cover a remote village's demand, LCOEs resulting in \$207/MWh [11]. Dawood et al. compared off-grid systems with PV, batteries and/or H<sub>2</sub> storage for a remote settlement demanding 2 MWh daily, where a hybrid energy storage system with both batteries and H<sub>2</sub> induced lowest costs of electricity with \$342/MWh. This more than halved the PV curtailment compared to coupling PV only with batteries [12].

We identify a number of research gaps in literature: First, to our knowledge, there is no similar study analyzing the design of a renewable energy system for a remote research facility in general and telescope in particular. Due to very different needs as well as environmental conditions study results from residential settings cannot be applied to telescopes. Further, studies on islanded, renewable-based energy systems have not been applied to high altitudes yet, only use a limited number of technologies and do not consider technology learning.

In this work we close these gaps by: 1. performing the first optimization of a power system for a remote telescope with a unique electricity demand, characterized by seasonal shifts and minimal day-night fluctuations. It serves as a pioneering example for the transition to RES in off-grid research facilities, crucial for reducing CO<sub>2</sub> emissions to meet climate targets. 2. considering elevation-specific derating factors serving as a first study in the design of high-altitude power systems. 3. providing a more comprehensive comparison of system setups based on renewable energy for remote and off-grid power systems: We evaluate the trade-offs between 100% renewable systems, and systems with fossil fuel backup, next to trade-offs between batteries and hybrid energy storage systems, offering insights into the most cost-effective and sustainable solutions. We compare systems using imported and on-site produced green H<sub>2</sub> to those only employing batteries. Concentrated Solar Power (CSP), a promising technology in high irradiation places, is compared to the more widely applied PV technology. 4. applying technology learning rates in a sensitivity analysis: In line with the projected start of AtLAST's operations in the early 2030s, we size a power system for 2030 with a wide range of cost decline assumptions in RES and varying fuel costs. In contrast to modeling the system with today's costs, the use of projected future costs paired with a cost-sensitivity analysis helps to better showcase relevant energy systems for AtLAST in the next decade in which it will need to be supplied. It thereby also represents a valuable case study for similar, remote infrastructure projects that are currently being planned.

Specifically, this work presents solutions to power AtLAST's consumption of annually ~7.7 GWh with an isolated power system, including business-as-usual powering with fossil fuel generation, and combinations of RES, energy storage and fossil fuel generation backup. We answer the following research questions:

1. Which system results in the lowest levelized costs of electricity (LCOE) to power the planned telescope?
2. How much more does it cost to use a power system without direct CO<sub>2</sub>e-emissions?
3. Which system setups are robust against uncertainty in future costs?

**2. Materials and methods**

We apply a cost-optimization model to find feasible power systems for the telescope, divided into eight scenarios:

1. Using diesel generators at 5000 m (Business-as-usual, BAU);
2. Combining PV and diesel generation (PV & Diesel, PVD)
  - at 5000 m (PVD↑);
  - at 2500 m (PVD↓);
3. Combining PV generation with a hybrid energy storage system
  - (a) with backup diesel generation (PV, Diesel & Energy Storage, PVDES)
    - at 5000 m (PVDED↑);
    - at 2500 m (PVDES↓);
  - (b) as a renewables-only system without diesel generation (Renewable Energy Sources, RES)

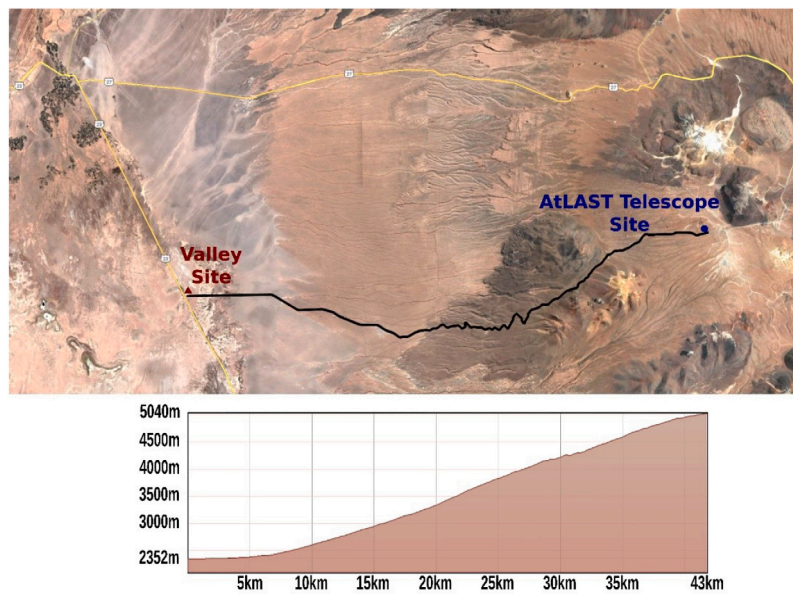


Fig. 1. Map of the studied area, highlighting a potential site of AtLAST, the power generation location in the valley and the necessary power line pathway between the two (see black line).

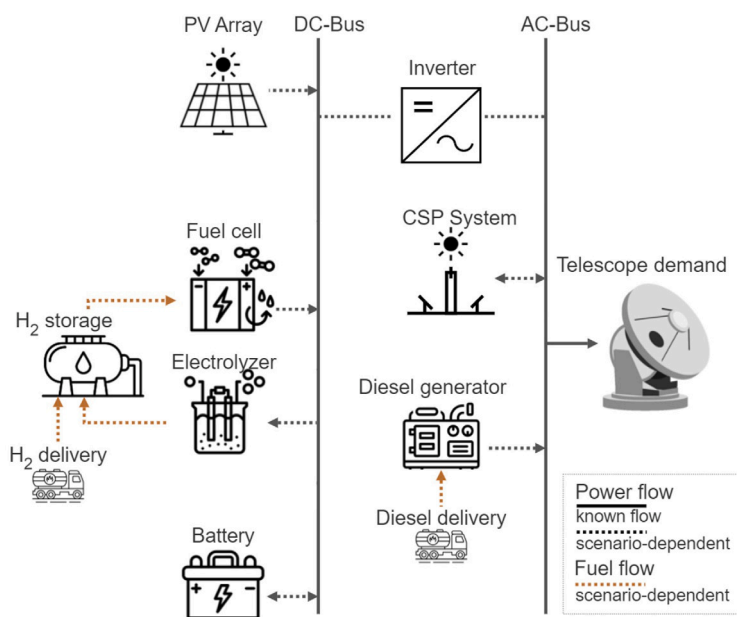


Fig. 2. Potential components of power system for the telescope, inverter not included in optimization.

- at 5000 m (RES↑);
- at 2500 m (RES↓);

4. Using CSP at an altitude of 2500 m (CSP).

2030 is set as the potential year to start operation. Location-wise, we consider systems built near the telescope on the Chajnantor plateau at ~5000 m and system at a Valley Site, 2500 m above sea level, see Fig. 1. For the telescope’s location, currently two options less than 5 km apart from each other are investigated. These are undistinguishable irradiation-wise, both present temperature variations from -20 to 10 °C and low pressures of ~550 Pa, for which we apply derating factors, and hence are considered alike in this work. The Valley Site, 43 km away from the telescope, implies less derating of components and easier access for operations, while adding costs for subterranean cabling. Only off-grid systems are considered.

To optimize the different scenarios, we apply highRES-AtLAST, an adaptation of the highRES model proposed by Price and Zeyringer for the energy system of Great Britain and Europe [13,14]. Constructed to design a cost-minimal power system using a linear programming model, it minimizes overall costs while meeting hourly demands and technical constraints. The main outputs are system costs, built capacities and hourly dispatch. We add a H<sub>2</sub> storage system with electrolyzers, storage and fuel cells and CSP as technologies to the model. The H<sub>2</sub> and CSP system (thermal energy) were implemented in terms of power (MW and MWh) to fit with the highRES structure. The limitations of highRES-AtLAST are the same as the original model. Fig. 2 shows an overview of all technologies in the system. 2030 serves as the demand and cost assumption year, while costs are set to inflation-adjusted real2022-US\$ [15]. Inputs for the model include solar generation capacity factors, Chilean component and fuel costs in 2030 and a demand

**Table 1**  
Demand estimation of AtLAST.

Demand constituent	Average demand (kW)	Peak demand (kW)
Cryogenic cooling	450	600
Telescope motors	350	1300
Heating, ventilation and air conditioning system	40	50
Electronics; instrument support; other	40	50

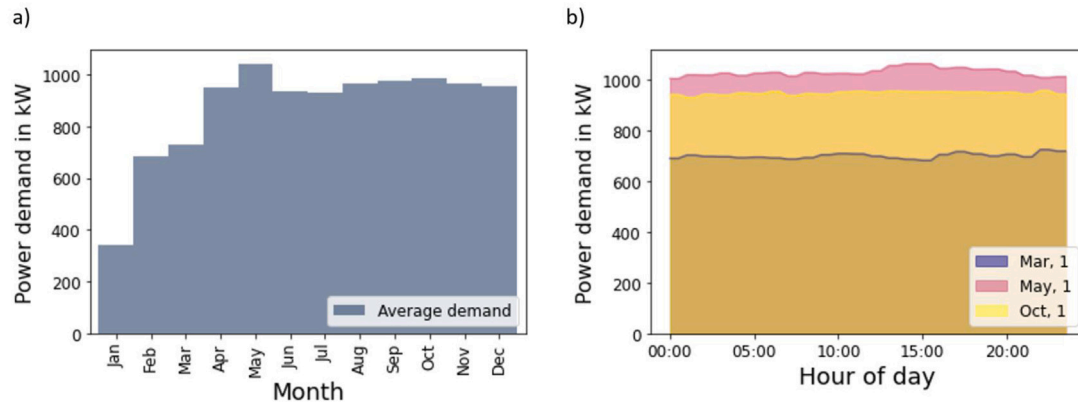


**Fig. 3.** Demand patterns of AtLAST in 2030, (a) average monthly demand; (b) exemplary daily demand curves.

time series for AtLAST. Different learning rates for component costs and variations in fuel costs are integrated via sensitivity analyses.

### 2.1. Estimating the telescope's demand

The demand of AtLAST comprises dish motors, a cryogenic cooling system for the instruments, electronics, instrument support, and a heating, ventilation, air conditioning system, see Table 1. Peak demands are supplied by supercapacitors outside the system presented. For the optimization, the historical demand of a smaller radio telescope is upscaled to match AtLAST's estimated demand, resulting in a one-year time series for 2030 at hourly granularity. Fig. 3(a) shows the estimated average monthly power demand, see Fig. 3(b) for exemplary daily demand curves.

### 2.2. Choice of system components

The global solar irradiation maximum lies within the Atacama Desert, an annual irradiation of  $\sim 2640$  kWh/m<sup>2</sup> can be assumed at the prospective sites [16,17]. As inputs for the optimization, we convert hourly irradiation values from ERA5, previously used to represent the weather conditions on a regional level in modeling the Chilean electricity generation [18], into capacity factors [17,19], see Fig. 4. While PV systems can be located at either 5000 m or 2500 m, CSP is excluded at the high site, to not interfere with astronomical observations. Wind power is not considered, as the areal average wind speed of 3.1 m/s is too low for power production [20].

To represent CSP in the model we consider three interlinked subsystems: the solar field (capturing solar irradiation), the thermal energy storage (storing surplus thermal energy), and the power block (generating power) [21]. We consider the two most established CSP technologies, the Parabolic Trough (PT) and the Solar Tower (ST) [22]. Advantages lie in their flexibility, as thermal energy storage allows for power generation on demand. However, CSP is often not competitive with the steeply declining PV costs, so some systems have been retrofitted to PV [23].

Today's telescopes in the area are for the majority supplied by diesel generators, which can ramp up and down flexibly and are dependent on regular refueling trucks. We employ similar diesel generators in our model.

#### 2.2.1. Energy storage systems

We consider both batteries and H<sub>2</sub> as energy storage technologies. In batteries, mature options include lead acid and lithium-ion (Li-ion) batteries. According to manufacturers, both technologies can withstand temperatures down to  $-20$  °C in discharge/storage, and down to 0 °C when charging. Lead acid batteries with their historically lower investment costs currently hold the leading role in stationary systems. In recent years, however, some found lower LCOEs with Li-ion batteries, based on their higher cycle life [24]. As additionally, Li-ion batteries perform better in life cycle assessments when compared to lead acid, we include only this technology in our setup [25].

When utilizing H<sub>2</sub> as an energy carrier in remote systems, two ways of operation are thinkable. For one, H<sub>2</sub> production off-site and shipment to the location is doable, requiring on-site storage and fuel cells to generate power. We only consider so-called green H<sub>2</sub>, stemming from RES-powered electrolysis. Without imported H<sub>2</sub>, the whole H<sub>2</sub> value chain is needed on-site, that is electrolyzers, H<sub>2</sub> storage and fuel cells. H<sub>2</sub> storage in stationary systems today is mostly conducted with compressed gas (CG) stored in steel cylinders at 50–700 bar [26]. MH applications for storing H<sub>2</sub> are investigated as a safer alternative to CG, e.g. by Endo et al. [9], but are not economically available yet.

#### 2.2.2. Derating factors

We do not know of any solar power system with a substantial energy storage system as proposed in this work in existence at 5000 m. In this techno-economical assessment, we consider technologies that could endure the harsh conditions of the location, and include derating factors to consider the low-pressure conditions at either site, see Table 2. These factors impact the components' power output. For instance, a diesel generator with a capacity of 2 MW at the AtLAST Site has a maximum effective capacity of 1 MW, that is its capacity multiplied with a derating factor of 0.5. Diesel generators are impacted by the less dense air, as less oxygen molecules are available for the burning process. Batteries are derated at altitudes, as the extremely low temperatures and low pressures represent an issue for their liquid electrolyte. Both electrolyzers and fuel cells are impacted by the lower amount of oxygen molecules available. The factors of diesel generators and batteries stem from empirical data and internal communications with experts from other telescopes in the areas. In experiments of Pratt et al. a PEMFC at an altitude of 2774 m had 6%–10% less stack voltage than its counterpart at an altitude of zero [27]. We hence assume similar derating factors for H<sub>2</sub> and batteries.



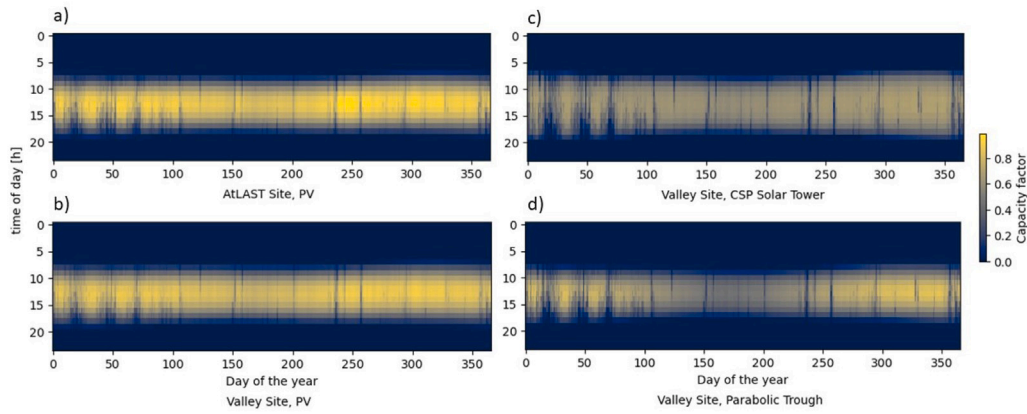


Fig. 4. Solar generation capacity factors: (a) PV at AtLAST Site, (b) at Valley Site, (c) CSP ST at Valley Site, (d) CSP PT at Valley Site.

Table 2  
Derating factors at 2500 and 5000 altitude meters.

System component	Derating factor at 2500 m	Derating factor at 5000 m
Diesel generator	0.75	0.5
Electrolyzer/Fuel Cell/Li-ion battery	0.95	0.8

Table 3  
Cost estimations in 2030, real2022-US\$ values.

Cost component	CAPEX	Unit	Lifetime
Monofacial monocrystalline PV	523 [28,29]	\$/kW <sub>p</sub>	
CSP solar field – PT/ST	209/148 [30]	\$/m <sup>2</sup>	
CSP thermal energy storage – PT/ST	37/19 [23,30,31]	\$/kWh <sub>th</sub>	25 years
CSP power block – PT/ST	869/1,156 [30]	\$/kW <sub>e</sub>	
Diesel generator	495 [32]	\$/kW	
Li-Ion batteries	262 [33,34]	\$/kWh	13 years [33]
Electrolyzer – Alkaline/PEM	434/483 [34]	\$/kW <sub>e</sub>	
CG H <sub>2</sub> storage	598 [35]	\$/kg H <sub>2</sub> stored	18 years [33]
PEMFC	1581 [36]	\$/kW <sub>e</sub>	
Subterranean power lines, 24 kV	23,599 [37]	\$/km	40 years

Table 4  
Sensitivity case cost estimations in 2030, real2022-US\$ values.

Cost component	Low case CAPEX	High case CAPEX	Unit
Monofacial monocrystalline PV	345 [28,29]	928 [38]	\$/kW <sub>p</sub>
Li-ion batteries	164 [33]	304 [34]	\$/kWh
Electrolyzer – Alkaline/PEM	247/327 [39]	774 [38]	\$/kW <sub>e</sub>
CG H <sub>2</sub> storage	286 [35]	780 [35]	\$/kg H <sub>2</sub> stored
PEMFC	1002 [40]	1876 [36]	\$/kW <sub>e</sub>

### 2.3. Component and fuel costs, sensitivity analysis

PV, batteries, and H<sub>2</sub> systems had a steep learning curve over the last decades, a trend forecasted to continue until beyond 2030, the planned building year of this system. In this work, we use Chilean forecasted costs, wherever possible, and integrate different learning rates in sensitivity analyses to account for variations in future component costs. The base case capital expenditures (CAPEX) and lifetime assumptions are shown in Table 3, with costs adjusted to real2022-US\$ values. See Table A.1 in Appendix for operational expenditures (OPEX). This optimization includes generation, storage units and long-distance cabling as the major cost components. Other electrical system components like inverters are not integrated, though they need to be considered in any final system design. Sensitivity analyses with costs as indicated in Tables 4 and 5 are performed to indicate the robustness of system setups against different learning curves and other fuel costs than the ones assumed in the base scenario.

#### 2.3.1. Power generation costs

In 2020, the median costs of Chilean PV systems > 1 MW<sub>p</sub> was at \$<sub>2020</sub>769/kW<sub>p</sub> (real2020-\$, inflation-adjusted US dollar value to

the year 2020) [28]. To forecast future costs we apply Vartiainen et al.’s base PV cost decrease rate of 39.3% from 2020 to 2030 on the Chile-specific costs, resulting in \$515.90/kW<sub>p</sub> in 2030 [28,29]. This is comparable with the International Renewable Energy Agency (IRENA)’s (2019) assumptions of \$<sub>2019</sub>340–834/kW<sub>p</sub> for utility-scale PV plants in 2030 [38]. For sensitivity cases, we include IRENA’s slow learning rate as our high, and the fast learning rate of Vartiainen et al. with a cost decrease of 59.4% as our low case sensitivity. See Table 4 for sensitivity case assumptions. Fig. 5 (a) shows the cost trajectories for PV and CSP.

With CSP, several studies report learning rates for this technology, though few present results based on future scenarios. The Joint Research Center forecasts a learning rate of 33% from 2015 to 2030 [45]. The Chilean Energy Ministry projects CSP cost decline of 23% in its carbon neutrality scenario [46]. Slower and faster learning rates range from 5%–49%. We adopt this Chilean carbon neutrality learning rate in our optimization, modularizing it on individual component costs from the National Renewable Energy Laboratory (NREL) [30]. CSP system costs in this work exceed those of PV and diesel-systems by far, so no sensitivity analysis is undertaken.

**Table 5**  
Fuel costs in 2030, base case and high-cost sensitivity, real2022-US\$ values.

Fuel	Base case costs	High case costs	Unit
Diesel	600.76 [41]	1,220.52 [42]	\$/m <sup>3</sup>
Green H <sub>2</sub>	1.13 [43]	1.40 [36]	\$/kg
Transporting H <sub>2</sub>	0.54 [44]		\$/kg/100 km

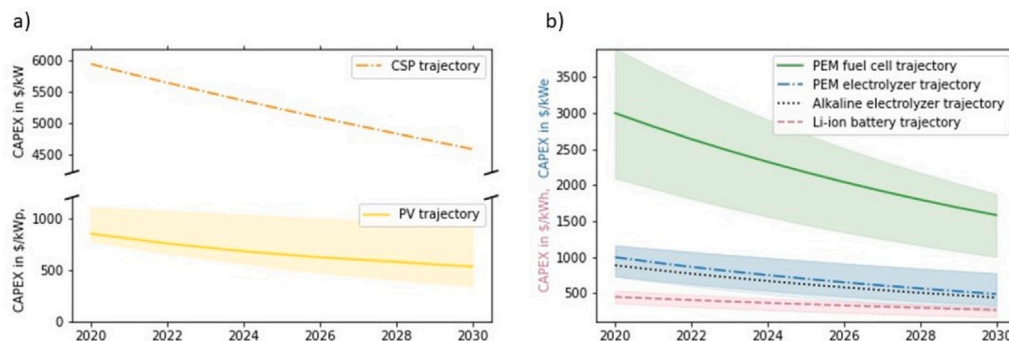


**Fig. 5.** Cost trajectory from 2020 to 2030 (a) for solar power generation, PV margins for cost sensitivities; (b) for energy storage components, margins for cost sensitivities.

### 2.3.2. Energy storage costs

By 2030, Li-ion costs are assumed to decline from 2020's \$<sub>2020</sub>350 to \$<sub>2020</sub>270/kWh or \$<sub>2020</sub>148–250/kWh by the US-American Department of Energy (DOE) and NREL, see energy storage cost trajectories in Fig. 5 (b) [33,34]. For our base case, we average between the medium NREL projections DOE's \$304/kWh, setting the value at \$262/kWh. The lower end of NREL's projection serves as the low and the DOE's normal assumption as the high sensitivity.

H<sub>2</sub> system cost decline projections are changing rapidly. In 2019, the International Energy Agency (IEA) assumed a technology-neutral decline in electrolysis costs from \$<sub>2019</sub>900/kW<sub>e</sub> down to \$<sub>2019</sub>700/kW<sub>e</sub> in 2030 [47]. The DOE (2020) assumed PEM electrolyzers costs to go down to \$393–481/kW<sub>e</sub> by 2030 [34]. In 2021, the Hydrogen Council and McKinsey & Company forecasted a decline from \$<sub>2021</sub>550–1050/kW<sub>e</sub> towards \$<sub>2021</sub>230–380/kW<sub>e</sub> in 2030 [39]. Industrial electrolyzer suppliers contacted by the authors expressed that CAPEX they see with vendors beat the recent literature predictions. We use the DOE's mean value as our base case at \$486/kW<sub>e</sub>, the Hydrogen Council's mean value of \$327/kW<sub>e</sub> as the low sensitivity, and the IEA's \$774/kW<sub>e</sub> as the high sensitivity case.

The more mature alkaline electrolyzer technology has lower investment costs than their PEM counterparts today, though Saba et al. foresee the costs of PEM systems approach those of alkaline electrolyzers soon [48]. We set base alkaline electrolyzer costs at the lower end of the DOE's PEM electrolyzer cost forecasts at \$434/kW<sub>e</sub> [34], and follow the lowest value of the Hydrogen Council for the low, the IEA's normal cost assumption for the high-cost sensitivity.

In CG H<sub>2</sub> storage systems, Sens et al. report costs of \$286–\$780/kg H<sub>2</sub> in 2030 [35]. Their mean value serves as our base case for CG, the lower and upper boundaries as the sensitivity costs. In stationary PEMFC costs, the European Union's Clean Hydrogen Partnership (2019) announced target cost declines from \$<sub>2019</sub>1900/kW<sub>e</sub> in 2020 to \$<sub>2019</sub>900/kW<sub>e</sub> in 2030 [40]. Cigolotti et al. (2021) expect cost drops from \$<sub>2021</sub>2000–3500/kW<sub>e</sub> to \$<sub>2021</sub>1200–1750/kW<sub>e</sub> by 2030 due to economies of scale [36]. We set their mean assumption as our base case. In the sensitivity analysis, the Clean Hydrogen Partnership's target serves as the low, with Cigolotti et al.'s upper value as the high case.

Uncertainties in the energy storage system comprise whether a big battery park is functional at the altitudes discussed and whether a green H<sub>2</sub> economy will develop until 2030. To find meaningful power system designs for AtLAST, we compare systems with hybrid energy storage against designs without a battery park or without H<sub>2</sub>.

### 2.3.3. Line and fuel costs

For Valley Site power systems, transmission lines need to be built to reach the ATLAST Site. We estimate 43 km of newly built 24 kV subterranean lines between the generation site and the telescope. Overhead lines are not applicable due to the sulfur-rich environment and harsh weather conditions. We apply costs from a Chilean contractor for subterranean lines plus a 30% surcharge for the remote and harsh conditions [37].

For the option of using off-site produced H<sub>2</sub>, we follow the Chilean government's (2021) assumption of \$<sub>2021</sub>1.05 per kg of green H<sub>2</sub> produced in 2030, based on analytics by McKinsey & Company [49]. IRENA (2022) expects costs of green H<sub>2</sub> in Chile of \$1.4/kg H<sub>2</sub> in 2030, which shall serve as our high sensitivity [42]. Following the work of Tashie-Lewis and Nnabuiife (2021), we consider \$<sub>2021</sub>0.50/kg/100 km for transporting H<sub>2</sub> in trucks [50]. We assume to import H<sub>2</sub> from the Pauna Solar park in María Elena weekly [44,51]. The trucking distance to the ATLAST Site is 250 km, to the Valley Site 200 km. All fuel costs are listed in Table 5.

With diesel, we are subject to volatile fossil fuel prices. 2022's peak Chilean diesel price was at \$1220.52/m<sup>3</sup>, nearly double the previous 4-year average of \$566.28/m<sup>3</sup> [52]. In private communications with the authors, Rystad Energy forecasted the Brent Crude Oil price to decline by 103% from 2022's high of \$122.71/b to \$60.40/b in 2030 [52]. Applying this ratio to the Chilean diesel price, we result in \$601/m<sup>3</sup> in 2030 in our base case. We include 2022's peak as the high sensitivity case. Shipping of diesel is included in the diesel generator OPEX, see Table A.1.

## 3. Results

The model highRES-AtLAST optimizes total system costs (annualized investment and dispatch costs). The results include the built capacity, dispatch, direct CO<sub>2</sub>e emissions from operation and the total electricity dispatch costs, amongst others. To calculate LCOEs of the system, the latter is divided by the annual demand of 7.7 GWh:

$$\text{LCOE} = \frac{\text{Annualized total electricity system cost}}{\text{Annual demand}}$$

In the following section, we discuss the base case scenario optimizations. We look at changing results when one energy storage option is excluded and further dive into costs from sensitivity analyses.

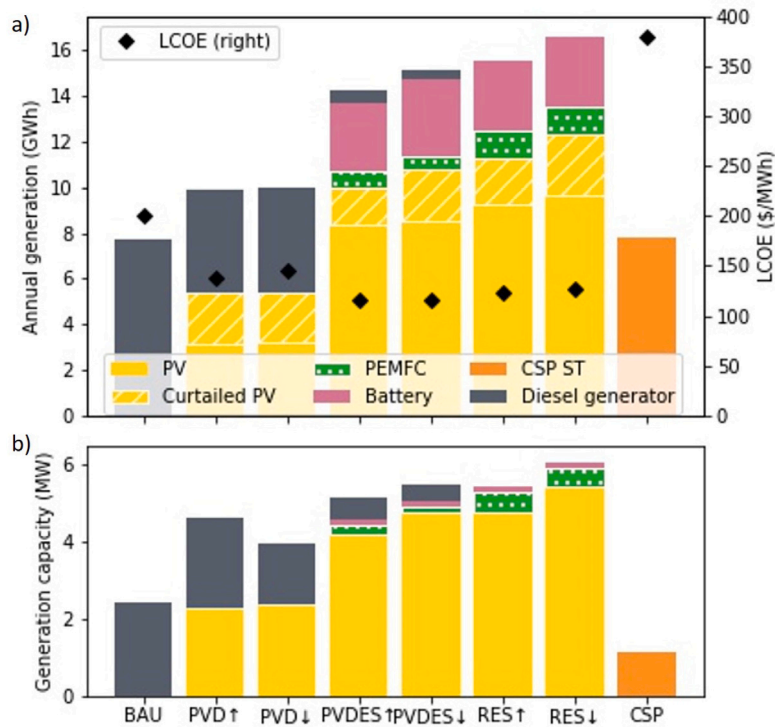


Fig. 6. Results base case: (a) Annual generation in GWh and LCOEs in \$/MWh, (b) built capacity in MW.

Table 6  
Direct CO<sub>2</sub>e emissions of the base case optimizations.

Scenario	BAU	PVD↑	PVD↓	PVDES↑	PVDES↓	RES↑	RES↓	CSP
Annual emissions (t CO <sub>2</sub> e/year)	6624	3892	3954	465	323	0	0	0
CO <sub>2</sub> e reduction compared to BAU (%)	–	41.20%	40.30%	93.00%	95.10%	100%	100%	100%

### 3.1. Base case optimized power systems

Fig. 6 shows the LCOEs, annual generation and built capacity of power generating units of the optimized scenarios, assuming costs as in our base case. See Table A.2 in Appendix for an extensive overview of the results. Scenarios with PV generation achieve LCOEs between \$116.0 and \$144.6/MWh. Employing PV together with energy storage solutions (PVDES and RES) results in lower generation costs than supplying the demand not covered by PV mostly with diesel generators (PVD). The lowest costs are achieved in PVDES, where the power system consists of PV, batteries, H<sub>2</sub> and diesel for backup. The PVDES and RES systems produce 51%–56% of their H<sub>2</sub> supply on-site, the rest is imported. When diving into the hourly generation data, we see that batteries and PEMFC generation are used throughout the nights of the simulated year, see Fig. 8. Power generation from diesel is mostly called during periods of less sunny days. The Chilean summer months January to March have enough solar generation and storage capacity to meet the seasonally lower telescope demand, while the autumn and winter months use generation from diesel for cloudy periods. When cutting out diesel generators in the optimization, LCOE values rise by 6–9 percentage points (pp.), including more generation from green H<sub>2</sub>. The CSP scenario results in LCOEs of \$379.5/MWh.

To evaluate the direct carbon footprint associated with the energy system in each scenario, we considered that only the diesel generator emits GHG during its operation. Assuming an emission factor of 0.86t CO<sub>2</sub>e/MWh [53], the direct GHG emissions, measured in CO<sub>2</sub>e, are highest in BAU, see Table 6. Pairing diesel with PV reduces the annual emissions by about 40%, while PVDES scenarios cut 93%–95% of the diesel-only emissions. Scenarios without diesel generators forego any direct emissions.

### 3.2. Systems without battery park or without green H<sub>2</sub>

Fig. 7 compares results from the base case PVDES and RES scenarios without a battery park and without H<sub>2</sub>. In cases without a battery park, resulting power systems mainly consist of PV and green H<sub>2</sub>. LCOEs range \$121–124/MWh with diesel as backup, and \$129–135/MWh without. A small capacity of batteries is built to balance frequency and voltage, assumed at 0.01MWh. The resulting systems in median produce 62% of the needed H<sub>2</sub> on-site. In the H<sub>2</sub>-based RES scenarios, an LCOE increase of 6pp. must be taken to reduce the final 13% of CO<sub>2</sub>e emissions from PVDES. The size of PV parks increases by 27%–42% compared to the base case with batteries, as more PV generation fuels electrolyzers. When cutting out H<sub>2</sub> as an option, results from the PVDES and RES scenarios change as shown in Fig. 7c. We see setups based on larger PV and battery capacities. The PV capacity in the RES scenarios increases by 28%–32%; with 44%–49% of its generation curtailed. LCOEs lie ~\$117/MWh when diesel serves as backup, and \$139–145/MWh without diesel in the system. In the RES scenarios without H<sub>2</sub>, LCOEs increase by 10 pp. compared to their PVDES counterpart. This saves the last ~8.6% of CO<sub>2</sub>e emissions which PVDES without H<sub>2</sub> emits.

### 3.3. Sensitivity analyses

Optimizing the power system with the sensitivity cost assumptions as in Section 2.3 results in varying system setups and costs. The resulting LCOEs are shown in Fig. 9, with the values resulting from the base case costs as black diamonds. In the H<sub>2</sub> systems high sensitivity,

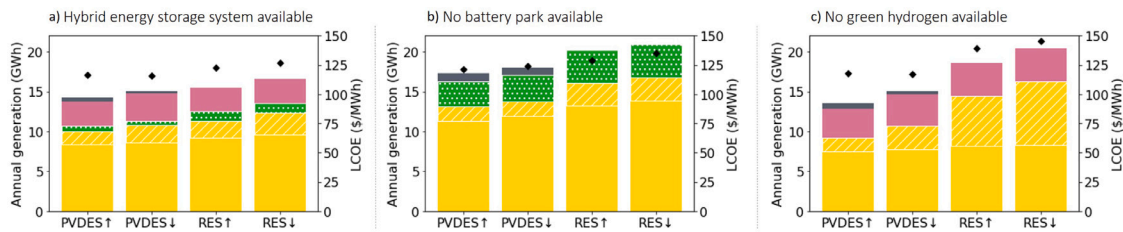


Fig. 7. Annual generation in GWh and LCOEs in \$/MWh: (a) Base case with hybrid energy storage, (b) base case without battery park, (c) base case without green H<sub>2</sub>.

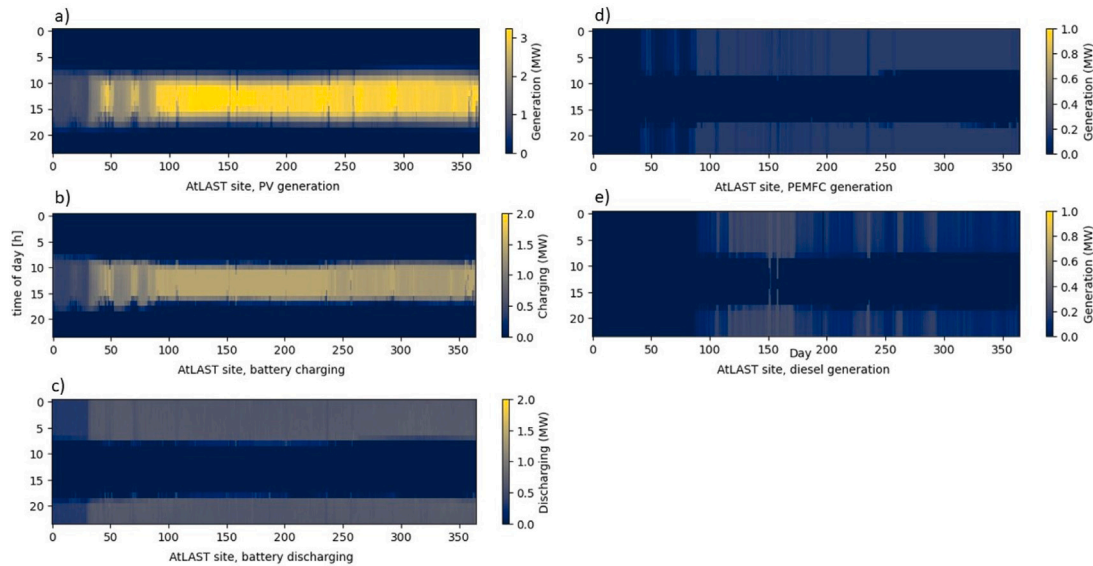


Fig. 8. Power generated and battery charging/discharging over optimized year, scenario PVDES↑: (a) PV generation, (b) battery charging, (c) battery discharging, (d) PEMFC generation, (e) diesel generation.

high costs of electrolyzers, fuel cells and imported green H<sub>2</sub> are applied coincidentally. In the low case, low costs of electrolyzers and PEMFC are used with base case green H<sub>2</sub> costs.

Higher fossil fuel costs lead to hefty LCOE jumps of 83% in the BAU scenario. Similar jumps of 70% are present in the PVD scenarios with high diesel costs, while PVDES only sees a cost increase of 3%. The scenarios with energy storage options, PVDES and RES, respond most to higher PV costs on the upper end. On the lower end, lower battery and lower H<sub>2</sub> system costs make the biggest difference on them.

#### 4. Discussion

All scenarios calculated result in systems that can cover the forecasted annual demand of the telescope AtLAST, as all optimizations converge to an optimal solution. Obtained LCOEs in the base case lie \$116–201/MWh, that is below up to a similar range to those of stationary systems for residential demanders discussed in Section 1. Lower generation costs in the power system setups presented are plausible given the cost decline assumptions applied, and pointing to the global solar maximum in the Atacama. Regarding our research questions, we find:

1. The base case cost assumptions lead to low LCOEs in PVDES and RES scenarios, with most of the generation carried by PV and batteries, next to some H<sub>2</sub>-driven fuel cells. Lowest costs with \$116/MWh are achieved in PVDES, with generators running on diesel used for cloudy days.

2. An all renewable power system as in RES↑ has LCOEs increase by 6% compared to PVDES↓. This small spike avoids the final 7% of the BAU scenario's emissions, equaling 465 t of CO<sub>2</sub>e, or 183 European researchers flying roundtrip to AtLAST (see CO<sub>2</sub>e emissions calculation with the Environmental Footprint 3.0 Method in Supplementary Material).
3. In the sensitivity analyses with upper and lower boundaries of expected costs in 2030, see Section 2.3, a jump above the base case cost value window of \$116–201/MWh presents itself in the diesel-only scenario. When applying the peak Chilean diesel price, system costs increase by 100% compared to the base case. It is deduced that a power system solely dependent on a fossil source of power generation leads to fickle power generation costs. We propose to employ a system with PV and applicable energy storage to power AtLAST sustainably, both in terms of GHG emissions, but also more robust costs.

GHG emissions related to the operation of the power system in scenarios swerving from the BAU approach reduce CO<sub>2</sub>e-emissions by 40 to 100%. PEM electrolyzers are preferred over alkaline ones, CSP ST is preferred over CSP PT. Systems that employ H<sub>2</sub> both use imported and on-site produced H<sub>2</sub>. The import is often used to cover H<sub>2</sub> demand peaks when high power demand meets cloudy weather.

Both systems without H<sub>2</sub> or without batteries were simulated to consider cases where these technologies cannot be considered for the telescope. This could e.g. occur in case the electrolyte of batteries does not operate well at the altitude, or in case green H<sub>2</sub> is not widely available as a fuel in 2030. Both instances result in more usage of diesel



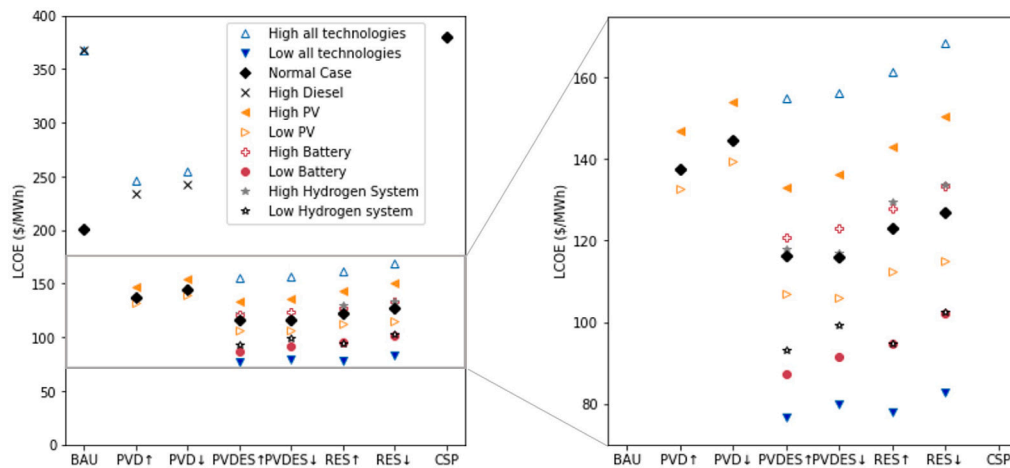


Fig. 9. LCOE comparison, base case costs (black diamonds) and sensitivity cost assumptions.

generation in PVDES, as seen in Fig. 7b and c. Not having batteries is slightly more expensive than not having H<sub>2</sub>. In RES, more PV capacity is needed to either supply a bigger battery park or electrolyzers. Decarbonifying the battery-rich systems without green H<sub>2</sub> results in high PV curtailments of up to 40%. Scenarios relying on PV and storage solutions generally resulted in lower costs than diesel-relying scenarios BAU and PVD, regardless whether batteries, green H<sub>2</sub> or a combination of the two are used. Low-CO<sub>2</sub>e emitting systems in PVDES need to install less PV and storage capacity than 100% renewable scenarios, resulting in lower costs and less curtailment.

Comparing PV and CSP systems, CSP presented costs of \$380/MWh, vastly higher than any PV scenario. With CSP costs forecasted as in this paper, this technology is not an economically viable option for AtLAST. To study the feasibility of this solar technology in larger systems, one could include additional demands, like neighboring telescopes or a nearby city, in future case studies.

#### 4.1. Weather data, climate change reliability

The solar capacity factors in this work were based on solely two ERA5 squares of 30 km<sup>2</sup>. With altitude changes from 2500 m to 5000 m, considerable variations in the weather conditions are expected. These cannot be represented within a single square grid, as the irradiation within is considered uniform. To better estimate the solar generation at the AtLAST and Valley Site, future work should consider the use of a higher resolution database.

For solar generation, we assumed the weather conditions for 2030 as similar to 2020. While estimations of solar variation expect the Chajnantor area to undergo no high changes in irradiation until 2065 [23], these small changes can be propagated during the system’s lifetime and affect its reliability. To design a reliable power system and reduce the uncertainty associated to weather data, a future climate scenario database could be considered in further investigations.

#### 4.2. High altitude considerations

This work considered both power systems next to the new telescope at an altitude of ~5000 m and systems down in the valley at ~2500 m, connected to the telescope via medium-voltage lines. The altitude made little difference to the resulting system costs, so that for example PVDES↑ and PVDES↓ both had LCOEs of \$116/MWh. While power systems at the Valley Site consider the costs of the line going up to the Chajnantor plateau, the derating factors and higher costs in imported H<sub>2</sub> increased costs at the high site. While cost-wise, building on either side is reasonable, we cannot be certain that the components considered can operate at the high altitude, as research in this area is lacking.

Testing on-site or in laboratory recreating the local conditions will help to answer this.

Further, snowfall needs to be considered at the AtLAST Site, as snow layers can reduce PV performance [54]. To account for this, higher OPEX due to snow handling could be introduced. Moreover, one could find best locations for PV arrays, that is sites with orography leading to less snow accumulation on the panels.

#### 4.3. Expanding the optimization: Life cycle assessment and energy communities

GHG emissions as presented in this paper include direct emissions only. When looking at the carbon footprint over the lifecycle of system components, indirect emissions from raw material sourcing, production, transport and end-of-life treatments should be considered as well, as RES incur indirect up- and downstream GHG emissions. This analysis is the topic of an upcoming paper in preparation by the authors. In this next work, we will include a life cycle assessment within highRES-AtLAST. Using a multi-objective optimization on both costs and lifecycle GHG emissions can generate a more profound answer to which systems induces lowest CO<sub>2</sub>e-emissions.

The systems presented are built to serve a single telescope with an annual demand of 7.7 GWh. In proximity to AtLAST on the Chajnantor plateau, eleven other telescopes are operating and could be integrated into a joint power system. This would not only reduce costs due to bigger scale, but also require less area and materials per generated Wh. A Valley Site power system, powering multiple telescopes on Chajnantor, would only require one power line to the plateau. One could moreover create an energy community with nearby localities, supplying excess power to locals.

### 5. Conclusions

The authors found lowest LCOEs of \$116/MWh for the telescope AtLAST with a power system employing a combination of PV, batteries, imported and on-site produced green H<sub>2</sub> with CG storage and PEMFC, and backup diesel. Compared to a business-as-usual setup with diesel generators only, systems based on PV present 31%–42% lower costs of power generation and more robustness regarding cost sensitivities. They save 40%–100% in direct GHG emissions compared to the BAU scenario. Systems running on 100% RES with hybrid energy storage have 6%–9% higher costs than those with additional diesel as backup. Setups where PV was used with only one main energy storage option, either batteries or H<sub>2</sub>, result in LCOE jumps of 1%–12%.

Synergies by building a centralized power system for the multitude of telescopes on the Chajnantor plateau could lead to lower costs,

**Table A.1**  
CAPEX and OPEX estimations in 2030, real2022-US\$ values.

Cost component	CAPEX	Unit	Fixed OPEX	Unit/year	Variable OPEX	Unit
Monofacial monocrystalline PV	523 [28,29]	\$/kW <sub>p</sub>	1% [29]	% of CAPEX	–	–
CSP Solar Field – PT/ST	209/148 [30]	\$/m <sup>2</sup>	57.35 [30]	\$/kWh	3.48/3.04 [30]	
Diesel generator	495 [32]	\$/kW	–	–	23.5 (10 [32] +0.5\$/1 for shipping (assumed))	\$/MWh
Li-Ion batteries	262 [33,34]	\$/kWh	0.43% [33]	% of CAPEX	0.5664 [33]	
Electrolyzer – Alkaline/PEM	434/483 [33]	\$/kW <sub>e</sub>	14.1 [33]	\$/kW <sub>e</sub>	0.9394 [33]	\$/MWh <sub>e</sub>
CG H <sub>2</sub> storage	598 [35]	\$/kg H <sub>2</sub> stored	2.1% [33]	% of CAPEX	–	–
PEMFC	1581 [36]	\$/kW <sub>e</sub>	14.1 [33]	\$/kW <sub>e</sub>	0.9394 [34]	\$/MWh <sub>e</sub>
Subterranean power lines, 24 kV	23,599 [37]	\$/km	0.5% (assumed)	% of CAPEX	–	–

**Table A.2**  
Results of base case cost optimization.

Scenario	Unit	BAU	PVD↑	PVD↓	PVDES↑	PVDES↓	RES↑	RES↓	CSP
Annualized total electricity system cost	k\$	1,544.7	1,059.9	1,112.8	894.9	893.3	946.1	978.0	2,921.6
<b>Capacity</b>									
Diesel	MW	2.40	2.34	1.58	0.58	0.43	–	–	
PV			2.27	2.38	4.20	4.76	4.75	5.44	
Alkaline electrolyzer	MW <sub>e</sub>				0.18	0.34	0.22	0.59	
PEM electrolyzer					0.68	0.39	1.01	0.91	–
CG storage	kg H <sub>2</sub>				263.1	159.8	1,048.7	1,399.3	
PEMFC	MW <sub>e</sub>	–	–	–	0.22	0.16	0.54	0.49	
Li-ion battery	MWh				15.1	14.2	15.2	12.4	
CSP solar field	MW								12.2
CSP ST									1.14
<b>Generation</b>									
Diesel	annual	7,697.6	4,523.5	4,594.9	540.8	375.2	–	–	
PV			3,174.2	3,203.4	8,404.0	8,544.4	9,217.7	9,627.1	
Thereof curtailed	MWh		2,223.9	2,183.5	1570.7	2,254.4	2,065.7	2,700.4	–
PEMFC					735.2	534.9	1,204.7	1,201.9	
Li-ion battery		–			2,993.7	3,396.4	3,015.9	3,052.4	
CSP solar field	MWh <sub>th</sub>		–	–					20,668.6
Thereof curtailed									2,815.0
CSP ST	MWh								7,798.1

e.g. in maintenance and cabling. Further research is needed to conclude whether the systems presented here can be employed at the altitudes discussed and what indirect emissions they entail. The open-source system design optimization of this work can also be applied for other (remote) facilities and thus serve as a lighthouse to astronomical observatories and off-grid stationary applications that would like to shift towards more sustainable power supply.

## Funding

This project has received funding from the European Union's Horizon 2020 research and innovation program under grant agreement No. 951815.

## CRediT authorship contribution statement

**Isabelle Violo:** Conceptualization, Methodology, Investigation, Data curation, Writing – original draft, Visualization. **Guillermo Valenzuela-Venegas:** Conceptualization, Methodology, Software, Investigation, Data curation, Writing – review & editing. **Marianne Zeyringer:** Conceptualization, Writing – review & editing, Supervision. **Sabrina Sartori:** Conceptualization, Writing – review & editing, Supervision, Project administration.

## Declaration of competing interest

The authors declare that they have no known competing financial interests or personal relationships that could have appeared to influence the work reported in this paper.

## Data availability

The highRES-AtLAST model is openly published. Restrictions apply to the availability of the demand dataset. A dummy demand dataset is available within the highRES-AtLAST model.

## Acknowledgments

We want to thank APEX for their kind collaboration. Special thanks goes to our astronomy colleagues Claudia Cicone, Carlos De Breuck and Tony Mroczkowski for the cooperation in this interdisciplinary project.

## Appendix A

See Tables A.1 and A.2.

## Appendix B. Supplementary data

Supplementary material related to this article can be found online at <https://doi.org/10.1016/j.energy.2023.128570>.

## References

- [1] Stevens ARH, Bellstedt S, Elahi PJ, Murphy MT. The imperative to reduce carbon emissions in astronomy. *Nat Astron* 2020;4(9):843–51.
- [2] Knödlseher J, Brau-Nogué S, Coriat M, Garnier P, Hughes A, Martin P, et al. Estimate of the carbon footprint of astronomical research infrastructures. *Nat Astron* 2022.

- [3] European Commission Statistical Office of the European Union. Energy, transport and environment statistics: 2020 edition. LU: Publications Office; 2020, URL <https://data.europa.eu/doi/10.2785/522192>.
- [4] Acohido A, Cavedoni C. Gemini Installs Record-Breaking Rooftop PV Solar Panel System | Gemini Observatory. 2017, URL <https://www.gemini.edu/node/12420>.
- [5] de Zeeuw T. Reaching New Heights in Astronomy - ESO Long Term perspectives. Messenger, ESO 2016;166:26.
- [6] Rodríguez F. ESO's Paranal Observatory starts receiving energy from the largest solar plant in Chile dedicated to astronomy. 2022, URL <https://www.eso.org/public/announcements/ann22010/>.
- [7] Klaassen PD, Mroczkowski TK, Cicone C, Hatziminaoglou E, Sartori S, Breuck CD, et al. The Atacama Large Aperture Submillimeter Telescope (AtLAST). In: Ground-based and airborne telescopes VIII, Vol. 11445. SPIE; 2020, p. 544–63. <http://dx.doi.org/10.1117/12.2561315>, URL <https://www.spiedigitallibrary.org/conference-proceedings-of-spie/11445/114452F/The-Atacama-Large-Aperture-Submillimeter-Telescope-AtLAST/10.1117/12.2561315.full>.
- [8] Ramasawmy J, Klaassen PD, Cicone C, Mroczkowski TK, Chen C-C, Cornish T, et al. The Atacama Large Aperture Submillimeter Telescope: key science drivers. In: Zmuidzinas J, Gao J-R, editors. millimeter, submillimeter, and far-infrared detectors and instrumentation for astronomy XI. Montréal, Canada: SPIE; 2022, p. 9, <https://doi.org/10.1117/12.2627505>, URL <https://www.spiedigitallibrary.org/conference-proceedings-of-spie/12190/2627505/The-Atacama-Large-Aperture-Submillimeter-Telescope-key-science-drivers/10.1117/12.2627505.full>.
- [9] Endo N, Shimoda E, Goshome K, Yamane T, Nozu T, Maeda T. Simulation of design and operation of hydrogen energy utilization system for a zero emission building. Int J Hydrogen Energy 2019;44(14):7118–24.
- [10] Ghenai C, Salameh T, Merabet A. Technico-economic analysis of off grid solar PV/Fuel cell energy system for residential community in desert region. Int J Hydrogen Energy 2020;45(20):11460–70.
- [11] Gebrehiwot K, Mondal MAH, Ringle C, Gebremeskel AG. Optimization and cost-benefit assessment of hybrid power systems for off-grid rural electrification in Ethiopia. Energy 2019;177:234–46.
- [12] Dawood F, Shafiullah G, Anda M. Stand-Alone Microgrid with 100% Renewable Energy: A Case Study with Hybrid Solar PV-Battery-Hydrogen. Sustainability 2020;12(5):2047.
- [13] Price J, Zeyringer M. highRES-Europe: The high spatial and temporal Resolution Electricity System model for Europe. SoftwareX 2022;17:101003.
- [14] Zeyringer M, Price J, Fais B, Li P-H, Sharp E. Designing low-carbon power systems for Great Britain in 2050 that are robust to the spatiotemporal and inter-annual variability of weather. Nat Energy 2018;3(5):395–403.
- [15] International Monetary Fund. World Economic Outlook (October 2022) - Inflation rate, average consumer prices, URL <https://www.imf.org/external/datamapper/PCPIPCH@WEO>.
- [16] Rondanelli R, Molina A, Falvey M. The Atacama Surface Solar Maximum. Bull Am Meteorol Soc 2015;96(3):405–18.
- [17] Hersbach H, Bell B, Berrisford P, Hirahara S, Horányi A, Muñoz-Sabater J, et al. The ERA5 global reanalysis. Q J R Meteorol Soc 2020;146(730):1999–2049, Publisher: John Wiley & Sons, Ltd.
- [18] Ramirez Camargo L, Valdes J, Masip Macia Y, Dorner W. Assessment of on-site steady electricity generation from hybrid renewable energy systems in Chile. Appl Energy 2019;250:1548–58.
- [19] Hofmann F, Hampp J, Neumann F, Brown T, Hörsch J. atlite: A lightweight Python package for calculating Renewable Power Potentials and Time Series. J Open Source Softw 2021;6(6):3294.
- [20] Muñoz RC, Falvey MJ, Arancibia M, Astudillo VI, Elgueta J, Ibarra M, et al. Wind Energy Exploration over the Atacama Desert: A Numerical Model-Guided Observational Program. Bull Am Meteorol Soc 2018;99(10):2079–92, URL <https://journals.ametsoc.org/view/journals/bams/99/10/bams-d-17-0019.1.xml>.
- [21] Chattopadhyay D, Bankuti M, Bazilian MD, de Sisternes F, Oguah S, Sanchez M. Capacity Planning Model with CSP and Battery. In: 2018 IEEE Power & Energy Society General Meeting (PESGM). Portland, OR: IEEE; 2018, p. 1–5. <http://dx.doi.org/10.1109/PESGM.2018.8586160>.
- [22] Răboacă MS, Badea G, Enache A, Filote C, Răsoi G, Rata M, et al. Concentrating Solar Power Technologies. Energies 2019;12(6):1048.
- [23] Schöniger F, Thonig R, Resch G, Lilliestam J. Making the sun shine at night: comparing the cost of dispatchable concentrating solar power and photovoltaics with storage. Energy Sour B 2021;16(1):55–74, URL <https://www.tandfonline.com/doi/full/10.1080/15567249.2020.1843565>.
- [24] Kebede AA, Coosemans T, Messagie M, Jemal T, Behabtu HA, Van Mierlo J, et al. Techno-economic analysis of lithium-ion and lead-acid batteries in stationary energy storage application. J Energy Storage 2021;40:102748.
- [25] Yudhistira R, Khatiwada D, Sanchez F. A comparative life cycle assessment of lithium-ion and lead-acid batteries for grid energy storage. J Clean Prod 2022;358:131999.
- [26] Egeland-Eriksen T, Hajizadeh A, Sartori S. Hydrogen-based systems for integration of renewable energy in power systems: Achievements and perspectives. Int J Hydrogen Energy 2021;46(63):31963–83.
- [27] Pratt JW, Brouwer J, Samuelsen GS. Performance of Proton Exchange Membrane Fuel Cell at High-Altitude Conditions. J Propuls Power 2007;23(2):437–44, <https://doi.org/10.2514/1.20535>.
- [28] NAMA Facility. Índice de Precios de Sistemas Fotovoltaicos (FV) conectados a la red de distribución comercializados en Chile. Technical report, Deutsche Gesellschaft für Internationale Zusammenarbeit (GIZ) GmbH: Sede de la Sociedad Bonn z Eschborn; 2020.
- [29] Vartiainen E, Masson G, Breyer C, Moser D, Román Medina E. Impact of weighted average cost of capital, capital expenditure, and other parameters on future utility-scale PV levelised cost of electricity. Prog Photovolt, Res Appl 2020;28(6):439–53, Publisher: Wiley Online Library.
- [30] Turchi CS, Boyd M, Kesseli D, Kurup P, Mehos MS, Neises TW, et al. CSP Systems Analysis - Final Project Report. NREL/TP-5500-72856, 1513197, 2019, <http://dx.doi.org/10.2172/1513197>, URL <http://www.osti.gov/servlets/purl/1513197>.
- [31] Dieckmann S, Dersch J, Giuliano S, Puppe M, Lüpfer E, Hennecke K, et al. LCOE reduction potential of parabolic trough and solar tower CSP technology until 2025. 2017, 160004, URL <http://aip.scitation.org/doi/abs/10.1063/1.4984538>.
- [32] Comisión Nacional de Energía. Informe de costos de tecnología as de generación. Santiago de Chile: Comisión Nacional de Energía; 2020, URL <https://www.ene.cl/wp-content/uploads/2020/03/ICTG-Marzo-2020.pdf>.
- [33] Cole W, Frazier AW, Augustine C. Cost Projections for Utility-Scale Battery Storage: 2021 Update. Technical Report NREL/TP-6A20-79236, Golden, CO: National Renewable Energy Laboratory; 2021, URL <https://www.nrel.gov/docs/fy21osti/79236.pdf>.
- [34] Mongird K, Viswanathan V, Alam J, Vartanian C, Sprengle V. 2020 Grid energy storage technology cost and performance assessment. Tech. rep., Tech. Rep., Pacific Northwest National Laboratory, US Department of Energy; 2020.
- [35] Sens L, Neuling U, Wilbrand K, Kaltschmitt M. Conditioned hydrogen for a green hydrogen supply for heavy duty-vehicles in 2030 and 2050 – A techno-economic well-to-tank assessment of various supply chains. Int J Hydrogen Energy 2022. S0360319922031275.
- [36] Cigolotti V, Genovese M, Fragiaco P. Comprehensive Review on Fuel Cell Technology for Stationary Applications as Sustainable and Efficient Poly-Generation Energy Systems. Energies 2021;14(16):4963.
- [37] CYPE Ingenieros SA. Precio en Chile de m de Línea subterránea de distribución de baja tensión directamente enterrada. Generador de precios de la construcción. 2022, URL [http://www.chile.generadordeprecios.info/espacios\\_urbanos/Instalaciones/Urbanas/IUB\\_Lineas\\_subterranas\\_de\\_baja\\_te/IUB020\\_Linea\\_subterranas\\_de\\_distribucion\\_d\\_0\\_0\\_0\\_0\\_1\\_0\\_0\\_0\\_0.html](http://www.chile.generadordeprecios.info/espacios_urbanos/Instalaciones/Urbanas/IUB_Lineas_subterranas_de_baja_te/IUB020_Linea_subterranas_de_distribucion_d_0_0_0_0_1_0_0_0_0.html).
- [38] International Renewable Energy Agency. Future of Solar Photovoltaic: Deployment, investment, technology, grid integration and socio-economic aspects (A Global Energy Transformation: paper). Technical Report, Abu Dhabi; 2019.
- [39] Hydrogen Council and McKinsey & Company. Hydrogen insights report 2021. Technical report, Brussels, Belgium: Hydrogen Council; 2021, URL <https://hydrogencouncil.com/en/hydrogen-insights-2021/>.
- [40] Partnership CH. Hydrogen Europe - strategic research & innovation agenda. Technical Report, Saint-Gilles, Belgium; 2019, URL [https://www.clean-hydrogen.europa.eu/about-us/key-documents/strategic-research-and-innovation-agenda\\_en](https://www.clean-hydrogen.europa.eu/about-us/key-documents/strategic-research-and-innovation-agenda_en).
- [41] Rystad Energy. Research inquiry about diesel / crude oil price in 2030. Private communication. 2022.
- [42] International Renewable Energy Agency. Global hydrogen trade to meet the 1.5° C climate goal: Part III– Green hydrogen cost and potential. Technical Report, Abu Dhabi; 2022, URL <https://irena.org/publications/2022/May/Global-hydrogen-trade-Cost>.
- [43] Endo N, Suzuki S, Goshome K, Maeda T. Operation of a bench-scale TiFe-based alloy tank under mild conditions for low-cost stationary hydrogen storage. Int J Hydrogen Energy 2017;42(8):5246–51.
- [44] Cabello L. Aprobación ambiental del parque Pauna, de 671 MWp, de Statkraft Chile. 2022, URL <https://www.pv-magazine-latam.com/2022/03/28/aprobacion-ambiental-del-parque-pauna-de-671-mwp-de-statkraft-chile/>.
- [45] European Commission Joint Research Centre. Cost development of low carbon energy technologies: scenario based cost trajectories to 2050, 2017 edition. LU: Publications Office; 2018, URL <https://data.europa.eu/doi/10.2760/490059>.
- [46] Ministerio de Energía, Gobierno de Chile. Planificación Energética de Largo Plazo 2023 - 2027: Informe Preliminar. Technical Report, Ministerio de Energía, Subsecretaría de Energía; División Políticas y Estudios Energéticos y Ambientales; Unidad de Planificación Energética y Nuevas Tecnologías; 2021.
- [47] Agency IE. The future of hydrogen. Technical Report, Paris: International Energy Agency; 2019, URL <https://www.iea.org/reports/the-future-of-hydrogen>.
- [48] Saba SM, Müller M, Robinus M, Stolten D. The investment costs of electrolysis – A comparison of cost studies from the past 30 years. Int J Hydrogen Energy 2018;43(3):1209–23.
- [49] Ministerio de Energía GdC. National green hydrogen strategy. Chile, a clean energy provider for a carbon neutral planet. 2021, URL [https://energia.gob.cl/sites/default/files/national\\_green\\_hydrogen\\_strategy\\_-\\_chile.pdf](https://energia.gob.cl/sites/default/files/national_green_hydrogen_strategy_-_chile.pdf).
- [50] Tashie-Lewis BC, Nnabuife SG. Hydrogen Production, Distribution, Storage and Power Conversion in a Hydrogen Economy - A Technology Review. Chem. Eng. J. Adv. 2021;8:100172, URL <https://linkinghub.elsevier.com/retrieve/pii/S2666821121000880>.
- [51] Statkraft. Statkraft ingresa a evaluación ambiental el proyecto solar más grande de Chile. 2022, URL <https://www.statkraft.cl/clientes/newsletter---statkraft-contigo/statkraft-contigo-nro-5/statkraft-ingresa-a-evaluacion-ambiental-el-proyecto-solar-mas-grande-de-chile/>.

- [52] Empresa Nacional del Petróleo. Inversionistas y Mercado - Relaciones Comerciales - Tabla de precios de paridad. 2022, URL [https://www.enap.cl/pag/66/1295/tabla\\_de\\_precios\\_de\\_paridad](https://www.enap.cl/pag/66/1295/tabla_de_precios_de_paridad).
- [53] Gaete-Morales C, Gallego-Schmid A, Stamford L, Azapagic A. Assessing the environmental sustainability of electricity generation in Chile. *Sci Total Environ* 2018;636:1155–70.
- [54] Santhakumari M, Sagar N. A review of the environmental factors degrading the performance of silicon wafer-based photovoltaic modules: Failure detection methods and essential mitigation techniques. *Renew Sustain Energy Rev* 2019;110:83–100.